Numerical Study of Droplet Evaporation in the Coupled High Temperature and Electrostatic Field

Ziwen Zuo, Junfeng Wang, Yuanping Huo, Yajun Fan
Jiangsu University
301 Xuefu Road, Zhenjiang, China
ivenzuo@gmail.com; wangjunfeng@ujs.edu.cn
huoyuanping@gmail.com; fanyajunjerry@gmail.com

Abstract -The numerical analysis of sessile droplet evaporation in the coupled high temperature and electrostatic fields is demonstrated. The joint of electrostatic field makes the inner flow of droplet more regular. But the velocity rates are decreased. Therefore, the evaporation rate is reduced. This is opposite to that of room temperature. The results provide a theoretic support for the application of spray dust for high temperature condition.

Keywords: High temperature, Evaporation, Electrostatic field, Droplet.

1. Introduction

The phenomenon of droplet evaporation in high temperature condition is not too far away from our daily life such as spilled water on the induction cooker. It is even more in industry from jet quenching to spray smoke dust. The operating temperature is higher than the boiling point in general, which makes some differences of droplet evaporation behavior compared with that of room temperature. Therefore these relevant problems become an interesting study direction. Renksizbulut et al (1983a, b) studied the droplet evaporation in a high temperature stream by both experimental and numerical methods. They provided a non-dimensional number-correlation for evaporation to determine whether the evaporation rate reduced. Harpole et al (1981) presented a stagnation-point solution to investigate the evaporation properties with more comprehensive affecting factors: blowing variable fluid properties, interdiffusion, and radiation. Beyond the pure academic studies, explores with industrial background seem more attractive due to the economic benefits. For lots simulation models, the calculating time are too long to be accepted. Abramzon et al (1989) developed a simple but sufficiently accurate model for spray combustion calculations. The radiation absorption becomes an important energy exchange when the work temperature is very high. Tseng et al (2005) numerically verified this factor.

When a droplet surrounded by the electrostatic field, special flow phenomenon is emerged. Together with evaporation process, the behaviors will become more complex and more valuable to explore. Hashinaga et al (1995) studied the evaporation of water under the electric field. They found that whatever alternating current direct currents could enhance the evaporation rate of the water liquid. Gamero-Castano (2002) found that within the evaporated mass, the emitted ion current is a very steep function of the electric field. Chen et al (2013) experimentally studied the initial spreading of a liquid drop under the electrostatic field. They found that the spreading dynamics was relative with electrolyte concentration and a simple mathematical model was proposed. Balachandran et al (2003) removed the smoke particles by using the charged water spray. The results showed that the removable efficiency of smoke particles for charged system is significantly higher than that of uncharged system. It should be noted that all these investigations are in the room temperature. In practice, the work condition is not always as low as this. For instance, the smokes from power plants are very high. How about the behaviors that presented from charged droplets in high temperature condition? Such problems are seldom reported in literatures. This paper based on boiling point evaporation model and leaky dielectric model (Taylor, 1966), use volume of fluid (VOF) free surface capture method (Hirt, 1981) to numerically investigation the charged water droplet evaporation under the coupled temperature and electrostatic fields. The most concern is how the electrostatic force influences the inner flow behavior of the evaporated droplet in the high temperature. The modeling results presented in this paper can be seemed as an electrohydrodynamic reference for the further exploration of the charged droplet

evaporates in high temperature condition.

2. Numerical Model and Mathematical Formulations

Figure 1 shows a 2D axisymmetric computational model for the problems to be studied here. We consider a hemispherical water droplet on an insulation board. A wall boundary above the droplet with a certain temperature works as the heat source to heat the phases. Other both sides are set as the outlets to exhaust conducted gas. The base plane connects with high electric potential and the above wall is grounded.
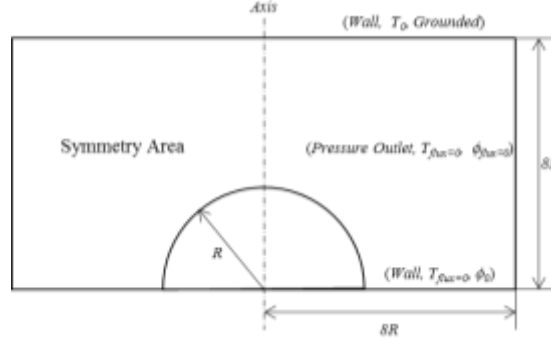
Fig. 1. Schematic of the axisymmetric model.

For a multi-field-phase mass transfer problem, we assume the fluids are immiscible and incompressible. The governing equations include mass conservation equation, N-S equation and energy equation.

$$\nabla \cdot \vec{U} = 0 \tag{1}$$

$$\frac{\partial \rho \vec{U}}{\partial t} + \nabla \rho \vec{U}^2 = -\nabla p + \nabla \cdot [\mu(\nabla \vec{U} + \nabla \vec{U}^T)] + F_E \tag{2}$$

$$\vec{F}_E = q^v \vec{E} - \frac{1}{2} \vec{E}^2 \nabla \varepsilon + \nabla(\frac{1}{2} \vec{E}^2 \frac{\partial \varepsilon}{\partial \rho} \rho) \tag{3}$$

Where, $\vec{U}$ is the velocity, ρ is the density, p is the pressure, μ is the viscosity, q^v is the volume charge density, ε_0 is the permittivity of vacuum, ε is the relative dielectric constant of the fluid. $\vec{E}$ is the electric field strength. The 3rd term on the right as electrostriction is ignored since it has no influence on the hydrostatics as the mass density in a liquid remains constant.

Consider that the wave motion of the interface significantly influences the inner flow of the droplet the surface tension coefficient (STC) is solved as a linear function:

$$y = 0.12179 - 1.6769 \times 10^{-4} x \tag{4}$$

The linear result is based on the follow table:

Table. 1. Surface tension coefficient of water.

Temperature /(K)	273	283	293	303	313	333	353	373
STC / (N/m)	0.0756	0.0742	0.0728	0.0712	0.0696	0.0662	0.0626	0.0589

Where y represents surface tension coefficient and x is the temperature.

A leaky dielectric model is used here to calculate the electric stress. The premise of this model is that the electric relaxation time of the fluid is much less than its viscous time: $t^E << t^v$, $t^E = \varepsilon / \sigma$, and $t^v = \rho L^2 / \mu$, where L is the characteristic length of the fluid. Namely, this assumption thinks that the free charges q^v in the fluid move to equilibrium almost instantly. Hence, eqs. (5) can be simplified as eqs.(6). The advantage of this theory is that the free charges moving resident property in the fluid evolution process is neglect, which greatly simplifies the complex charging process.

$$\frac{Dq^v}{Dt} = \frac{\partial q^v}{\partial t} + \vec{U} \cdot \nabla q^v = -\nabla \cdot (\sigma \vec{E}) \tag{5}$$

$$0 = \nabla \cdot (\sigma \vec{E}) \tag{6}$$

In the liquid-gas multiphase flow system, the liquid phase is easily satisfies the above premise, but this assumption is not established in the gas phase. Consider that the physical properties inside the evaporating drop are the most concerns, and the gas flow effects inside droplet are weak, the electric stress is calculated only on the liquid phase as well as the interface. Moreover, if the stress works on the gas phase, some unexpected perturbations will appear which make the interface does extra waves. That because in real terms, the free charges diffuse in the gas flow is much slower than that in liquid. Before they reach the equilibrium condition, the gas is already moves pass. Therefore, the majority charges are gathering near the interface with a typical thickness. Approximately, the electric stress is neglect in the gas phase, but the electrostatic field is calculated in both phases to get a continuous field distribution.

The electric field intensity $\vec{E}$ in eqs. (6) is satisfies:

$$\vec{E} = -\nabla \phi \tag{7}$$

Substitute this equation for eqs. (6), the electrostatic field formula can be expressed as:

$$\nabla \cdot (\sigma \nabla \phi) = 0 \tag{8}$$

The electrostatic field distribution can be obtained from eqs. (8), then electric field intensity $\vec{E}$ will be calculated. The volume charge density can be obtained through eqs. (9):

$$q^v = \nabla \cdot (\varepsilon \vec{E}) \tag{9}$$

By solving above parameters, the electric stress for constant density fluids system can be obtained by eqs.(10):

$$\vec{F}_E = -\frac{1}{2} \vec{E} \cdot \vec{E} \nabla \varepsilon + q^v \vec{E} \tag{10}$$

The energy equation is solved as:

$$\rho c_p \frac{DT}{Dt} = \nabla (k \nabla T) + \frac{Dp}{Dt} + S_{evap} \tag{11}$$

The coupled temperature and electrostatic multi-field mass transfer system is a rather complex interacting event. Based on the key concern of the liquid phase evolution characteristics, the evaporation process is simplified. Specifically, the product produced by the water evaporation is considered as air rather vapor in this simulation, which can avoid the calculation that mass, energy and charges diffuse between multicomponent phases. In addition, if multicomponent phase condition is considered, the fluid physical properties must be changed which would case lots chain effects such as the conductivity. Other, the vapor diffusion rate in air is very fast under the high temperature field. Compare with surrounding air, the amount of vapor is so small that can be neglect.

The mass transfer of the fluid is determined by the equation:

$$m = coeff \cdot \alpha \rho_l \frac{(T - T_{sat})}{T_{sat}} \tag{12}$$

Where *coeff* is an experienced parameter and the value is 0.1 (Lee, 1980).

Then the source term S_{evap} can be expressed as:

$$S_{evap} = -m \cdot L_{LHV} \tag{13}$$

The minus on the right side of the equation means evaporation is an endothermic process.

To capture the free interface of the droplet and ambient air, a volume of fluid method (VOF) is used in this paper. The physical parameters are linear interpolated on the interface such as:

$$\left. \begin{aligned} \rho &= \alpha \rho_{liq} + (1-\alpha)\rho_{gas} \\ \varepsilon &= \alpha \varepsilon_{liq} + (1-\alpha)\varepsilon_{gas} \\ \sigma &= \alpha \sigma_{liq} + (1-\alpha)\sigma_{gas} \end{aligned} \right\} \tag{14}$$

3. Results and Discussion

We consider the case that a hemispherical water droplet with $0.1mm$ radius and $303K$ temperature on the insulation board, the contact angle is set for $90°$. A pair of parallel plates induces a uniform electrostatic field which influences the droplet evaporation. Firstly the droplet is suddenly put into the system surrounded by the $500K$ air. Thermal radiation is not considered. The extreme temperature difference on both sides of the interface leads to the droplet surface shakes in high frequency. A deeper explanation is that the temperature gradient changes the local surface tension which breaks the pressure balance on sides of the droplet. This gradient is so high that induces the violent pressure variation.

Figuer 2 shows the evaporation flow field at $20ms$. The temperature gradient cross the interface leads to an emergence of Marangoni stresses that promotes the symmetry flow circles inside the droplet. Together with the circle flows, the isotherms are embedding in to the droplet as wedge shape along the axis. The worth noticeable thing is that the isotherms are not smooth. From the flow vector field, we can find some small vortexes near the bottom of the inner surface. A thin boundary line is formed outer the edge of the vortexes which stops the advance of the isotherms. Moreover, some vortexes also exist near the outer interface. When put a room-temperature droplet suddenly into the high temperature air field, the heated interface begins to evaporate and then the latent heat of water evaporation takes out energy which in turn pulls down the ambient temperature as shown in Figure 3. The generated gas spreads to form Stefan flows. It is well know that the gas flows from hot areas to where cool, hence in this case the air flows from top plane to the interface and meets the Stefan flow there. The mixed streams are amplified by the shake of the interface results in the vortexes formed outside the droplet surface.
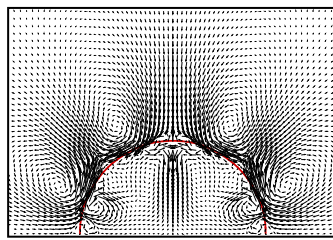
Fig. 2. Evaporation flow field at $20ms$.
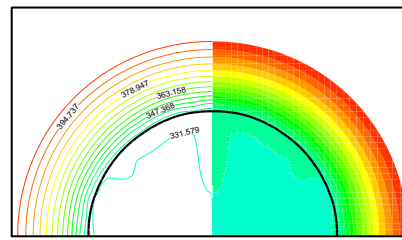
Fig. 3. Isotherms at $20ms$.

As time goes on, some bubbles appear in the droplet. In Figure 4 , a spot can be seen at the location where the axis crosses with the base plane. That is a forming bubble. The hot air heating the droplet to boiling point by overcome the latent heat of vaporization. Thinking only from the flow aspect, the lower velocity rate the bubble easier appears. Figure 5 demonstrates the axis velocity rate inside the droplet at $66.9ms$. The velocity approachs to zero where the axis coordinate close to zero. Hence, this is a region where the bubbles likely to arise. In addition, the bubbles appear and come up disturb the orgnized Marangoni flow pattern, which makes the droplet disintegrate vulnerably.
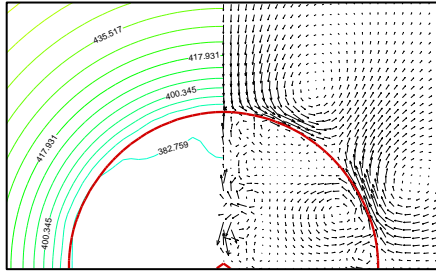
Fig. 4. Bubble appears at 66.9*ms* .
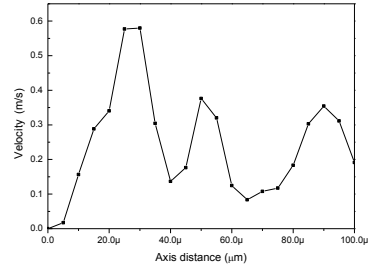
Fig. 5. Flow velocity rate along axis at 66.9*ms*.
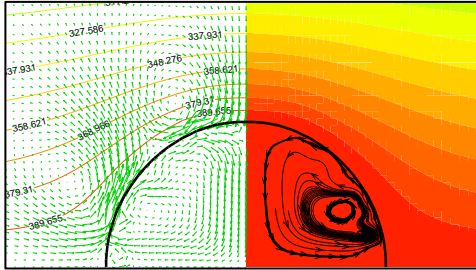
Fig. 6. Inner flow pattern of the charged droplet (500*kV/m*).
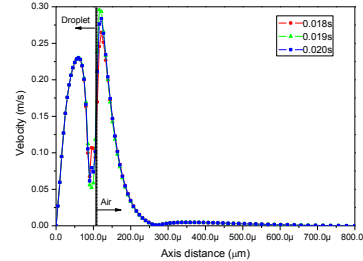
Fig. 7. Flow velocity rate along axis (500*kV/m*).

When the electrostatic field works on the droplet, electric stress drives the liquid does circle motion. After a period of time, the electric stress are balanced by the viscous force, the flow keeps a relatively stable state and the droplet deforms slightly as shown in Figure 6. If we scrutinize Figure 7 we can find that the velocity near the 100μm vertical dotted line has some fluctuations. That means the electric stress promotes the shake of the interface in high frequency (about 1000Hz). The flow pattern near the outer surface is similar with that of evaporation. As mentioned above, the electric stress is not calculated in air. Therefore, this flow is induced only by the variation of the interface. Compared with evaporation condition, we can find that the changes of droplet surface are an important element which affects the outer flow.

Because the conductivity of water is far greater than ambient air, the inner flow of droplet is from the vertex to the bottom, completes a circle along the interface. This circle direction is similar with that of evaporation. Hence, we concern about how the evolution of an evaporated droplet with the joint of electrostatic field. With this concern, we obtain a velocity diagram of the inner droplet as shown in Figure 8. It is weird that the velocity rate line of coupled fields is the lowest one. In our previous prediction, the superposition of two similar flows could enhance the inner flow rate of the droplet, which promotes the energy transport from interface to inner region. Therefore, the evaporation rate is indirectly increased. This prediction is based on the room temperature conditions. But for high temperature condition, results are in the opposite direction. Therefore, we need to analysis the inner flow behaviors of the droplet to find the answer.
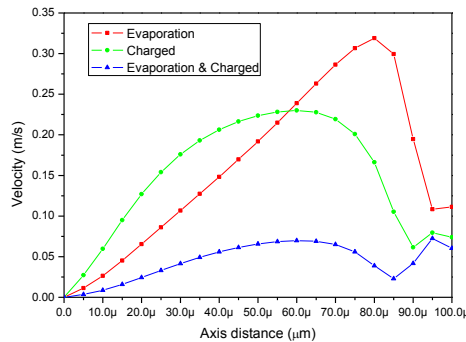
Fig. 8. Flow velocity rate along axis (20*ms*, $\vec{E}$: 500*kV/m*).

The flow fields of both single temperature and coupled electrostatic fields at the beginning evaporation period are exhibited in Figure 9. Unlike room temperature evaporation, the stream patterns in high temperature condition begin with three main vortexes rather than a whole one. These changes are caused by the nouniform distribution of the surface tension and inner pressure difference. Over time,

these vortexes merge together gradually before bubbles coming. During this process, the velocity in the droplet is not always increases. We monitor the axis velocity of the droplet and draw a diagram in Figure 10(a). In this diagram, the 0.05s curve is lower than that of 0.04s. The fusion of the vortexes leads to the loss of momentum which reduces the velocity in the droplet. When a whole vortex pattern forms, the velocity rate rises as the droplet temperature rising.

When electrostatic field joins in the evaporation system, the electric force makes some difference compared with single temperature cased evaporation flow structure as shown in Figure 9(b). At the very beginning, the electric force overcomes the stresses caused by the variation of the surface tension and pressure difference to guide the flow moves as a single circle. Du to low cycling speed, the stress variations flatten the outer edge of the vortex seems as a pit. From an overall flow region inner droplet, the charged stream lines always keep certain regular structure. This characteristic is conducive to the morphology stabilization of the droplet. The evaporation model is based on boiling point mass transfer theory. Therefore, the diffusion evaporation under the boiling point is not considered. That means the temperature on the interface must reach the boiling point then the mass transfer happens. This approximation provides a relatively stable droplet surface to more accurately compare the inner flow behaviors for different work conditions.

In the coupled fields, the electric stress needs to fight against the stresses from surface tension, pressure and temperature. The cost of this process is the loss of momentum just as the vortexes evolution in the single evaporation process. Lower momentum means lower velocity rates as shown in Figure 8. Hence the flow rate under the coupled fields is lower the other two. Not like the stresses caused by the temperature difference, the electric stress works immediately as soon as the electrostatic field joins in. And, this effect always keeps a relatively certainty strength to maintain the stable flow structure. The needed energy is complemented from the applied electrostatic field.
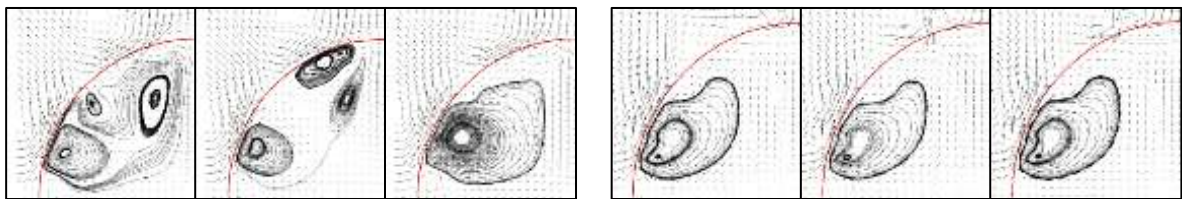
(a): Single temperature field (40ms, 50ms, 60ms)   (b): Coupled fields (10ms, 40ms, 60ms, $\bar{E}$: 500kV/m)
Fig. 9. Inner flow pattern of the droplet.
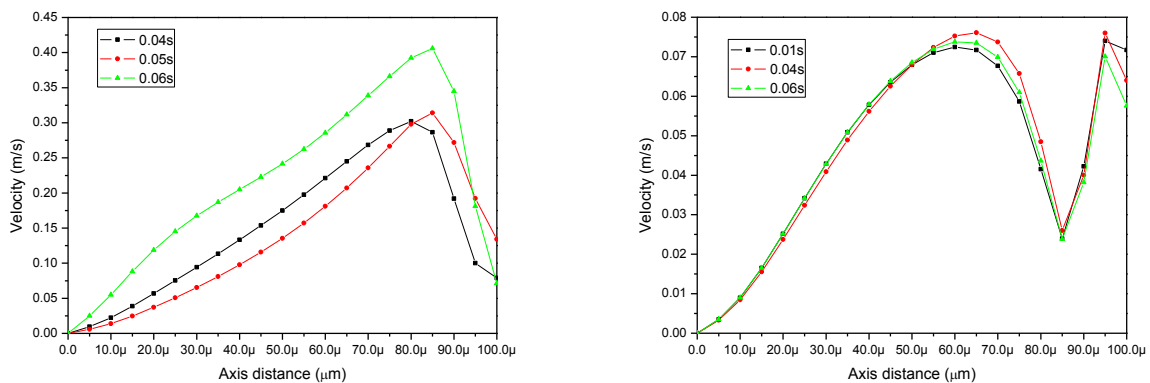
(a): Single temperature field   (b): Coupled fields ($\bar{E}$: 500kV/m)
Fig. 10. Flow velocity rate along axis.

(a): Coupled fields ($\vec{E}$: 20kV/m) (b): Coupled fields (70ms)

Fig. 11. Flow velocity rate along axis.

← (a): $\vec{E}$: 20kV/m
10ms, 40ms, 60ms

↓ (b): 70ms
$\vec{E}$: 20kV/m, 50kV/m, 100kV/m
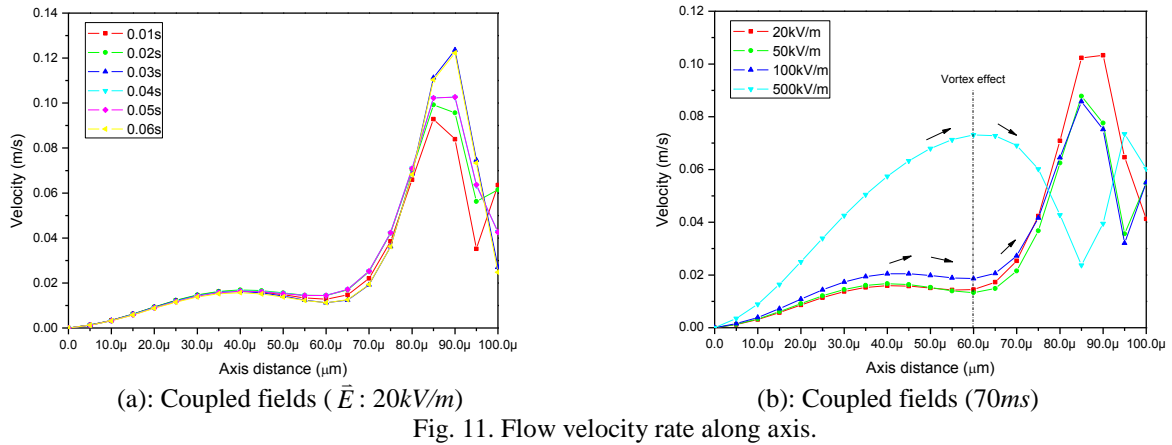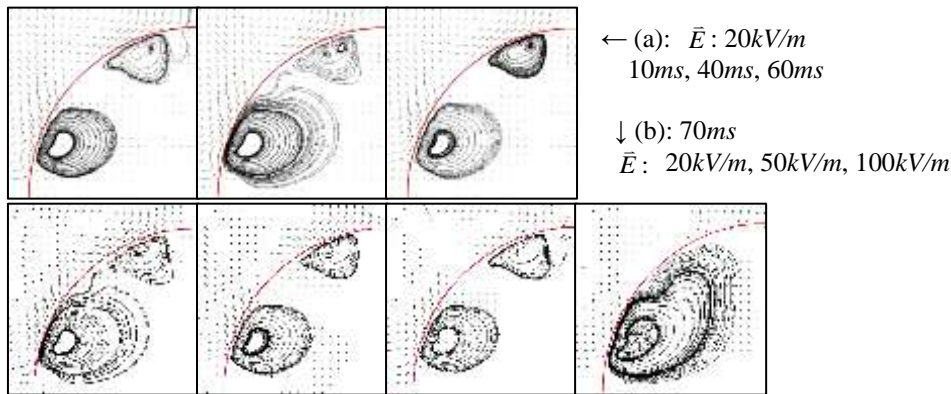
Fig. 12. Inner flow pattern of the droplet.

Restrained by the stable electrostatic field, the velocity rate in the droplet keeps nearly constant even the electrostatic field intensity is very low as shown in Figure 11(a). Obvious fluctuations are located closely to the interface (80μm~100μm). But, under lower electrostatic field intensity, more than one main vortex is exists in the droplet as shown in Figure 12(a). The electric stress is not strong enough to turn around the vortex which closer to axis. When the field intensity is powerful enough, the vortexes fuse tighter as a whole one as shown in Figure 12(b). Through the analysis of the inner flow behavior of droplet, the different velocity trend between Figure 10(b) and Figure 11(a) can be explained. The axis velocity data in Figure 12 are extracted and used to make a diagram as shown in Figure 11(b). From this diagram, we can clearly find that the 500kV/m line first rises and then falls while the other three are continue to increase. Combining with Figure 12, the distance for axis to the vortex is first near then far. The rotation effect is directly determined by the distance away from the vortex center zone. The closer the point to vortex, the faster fluid becomes. For other three, the extra vortex works as a relay station though the directions of rotation are opposite.

Because the flow cycle is starts from equator to the center point that temperature distributions on the axis can be used to estimate the droplet temperature. The temperature distributions on the axis of 500K and 500K-500kV/m work conditions from 10ms to 60ms are shown in Figure 13. The curves seem very flat, that means the velocity differences on the axis have small impact to the temperature distribution. The temperature evolution of center point before 65ms under deferent work conditions are demonstrated in Figure 14. The temperature gradients of charged droplets are almost the same. By the offset of the stresses from temperature difference and fluid properties, the electric stress is sharply cuts down and thus the so driven flow rate is lower. In addition, the mix rate of the regular flow pattern is lower than that of single evaporation flow pattern. All these lead to the slowly increase of the temperature in the charged droplets.
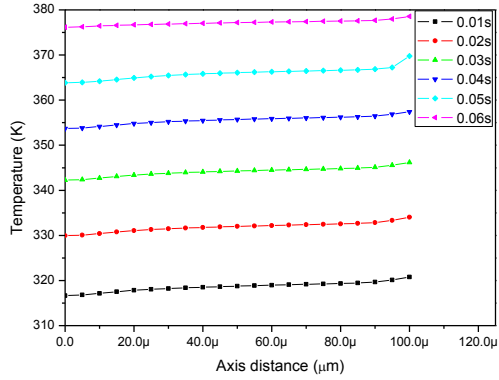
(a): 500*K*, uncharged
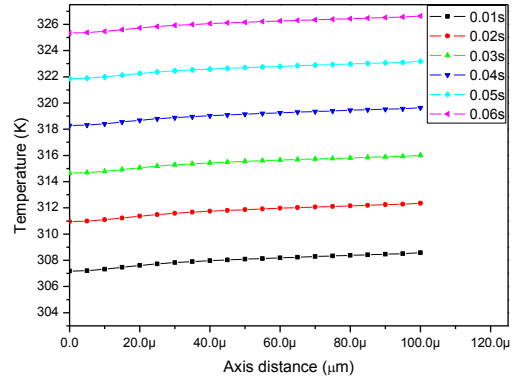
(b): 500*K*, $\vec{E}$: 500*kV/m*

Fig. 13. Temperature distribution along axis.
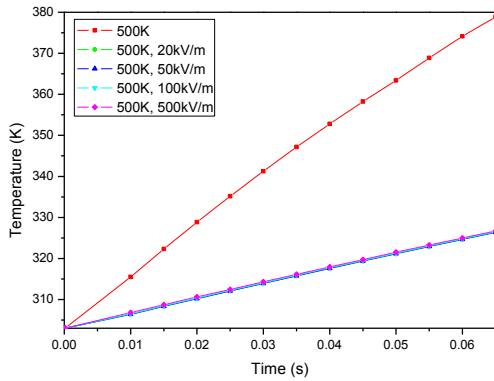
Fig. 14. Temperature distribution (center point).
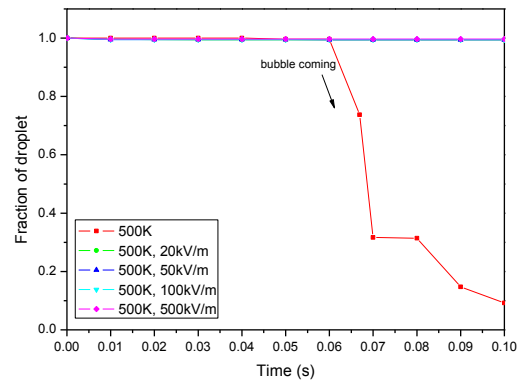
Fig. 15. Evaporation rate of the droplet.

Figure 15 shows the evaporation rate of droplet under different electric field intensities. The uncharged line shows that when a bubble generating, the evaporation rate increased sharply. As the substrate is heated to the boiling point, the base of the droplet is unstable, finally the coming of the bubble make the evaporation line unsmooth. Compared with uncharged condition, the temperature rising rates of the charged ones are much smaller. This leads to a lower evaporation rate for charged systems. For our calculation, there is no bubble comes even 300*ms* pass over. Though more time steps are iterated, the errors may become much obvious. That because the radiated heat transfer and the diffusion of mass transfer under the boiling point is neglect. Long calculating time duration can accumulate these errors to unacceptable levels.

4. Conclusion

The evaporation of a sessile droplet under the coupled high temperature and electrostatic field is simulated. In single high temperature condition, the inner flow is not as same as that under the room temperature. Three main vortexes are formed at the very beginning. Latter, they merged into a whole one. When electrostatic field joins in, the inner flow behavior is changed. An entire vortex occupies the inner region from the initial time. The inner flow velocity rates always keep a certain level and increase with the electric field intensity. Due to the suppression of the production of more vortexes, the electric stress is fight against with surface tension and other stresses caused by the temperature gradient. That leads to the loss of momentum. Therefore, the velocity rates in coupled fields are lower than that of single high temperature condition. According that, the temperature increase rate of the charged droplet is reduced. Then the evaporation rate of the charged droplet is reduced. In addition, the time of bubble coming is delayed.

References

Abramzon B., Sirignano W.A. (1989). Droplet vaporization model for spray combustion calculations[J]. International journal of heat and mass transfer, 32(9), 1605-1618.

Balachandran W., Jaworek A., Krupa A., et al. (2003). Efficiency of smoke removal by charged water droplets[J]. Journal of electrostatics, 58(3), 209-220.

Chen L., Li C., van der Vegt N. F. A., et al. (2013). Initial electrospreading of aqueous electrolyte drops[J]. Physical review letters, 110(2), 026103.

Gamero-Castano M. (2002). Electric-field-induced ion evaporation from dielectric liquid[J]. Physical review letters, 89(14), 147602-147602.

Harpole G. M. (1981). Droplet evaporation in high temperature environments[J]. Journal of Heat Transfer, 103(1), 86-91.

Hashinaga F., Kharel G.P., Shintani R. (1995). Effect of Ordinary Frequency High Electric Fields on Evaporation and Drying[J]. Food Science and Technology International, Tokyo, 1(2), 77-81.

Hirt C.W., Nichols B.D. (1981). Volume of fluid (VOF) method for the dynamics of free boundaries[J]. Journal of computational physics, 39(1), 201-225.

Lee W.H. (1980). Pressure iteration scheme for two-phase flow modeling[J]. IN" MULTIPHASE TRANSPORT: FUNDAMENTALS, REACTOR SAFETY, APPLICATIONS", 407-432.

Renksizbulut M., Yuen M.C. (1983). Experimental study of droplet evaporation in a high-temperature air stream[J]. Journal of heat transfer, 105(2), 384-388.

Renksizbulut M., Yuen M.C. (1983). Numerical study of droplet evaporation in a high-temperature stream[J]. Journal of Heat Transfer, 105(2), 389-397.

Renksizbulut M., Nafziger R., Li X. (1991). A mass transfer correlation for droplet evaporation in high-temperature flows[J]. Chemical engineering science, 46(9), 2351-2358.

Taylor G. (1966). Studies in electrohydrodynamics. I. The circulation produced in a drop by electrical field[J]. Proceedings of the Royal Society of London. Series A. Mathematical and Physical Sciences, 291(1425), 159-166.

Tseng C.C., Viskanta R. (2005). Effect of radiation absorption on fuel droplet evaporation[J]. Combustion science and technology, 177(8), 1511-1542.